FAS http://e-fas.org
Fisheries and Aquatic Sciences

Original Article
Fish Aquat Sci 18(1), 89-98, 2015

Chitosan-Coated Fe_3O_4 Magnetic Nanoparticles as Carrier of Cisplatin for Drug Delivery

Yosefine Arum[1], Yun-Ok Oh[2,4], Hyun Wook Kang[2,4], Seok-Hwan Ahn[3] and Junghwan Oh[2,4]*

[1]Testing Center for Product Quality, Ministry of Trade Republic of Indonesia, Jakarta 13740, Indonesia
[2]Department of Biomedical Engineering, Pukyong National University, Busan 608-737, Korea
[3]Department of Mechatronics Engineering, Jungwon University, Geosan 367-700, Korea
[4]Center for Marine-Integrated Biotechnology (BK21 Plus), Pukyong National University, Busan 608-737, Korea

Abstract

A synthesis method for a chitosan-coated magnetic drug-delivery system of cisplatin is proposed. Here, cisplatin was conjugated to the surface of Magnetite (Fe3O4) nanoparticles via a (3-Aminopropyl)-trimethoxysilane (APTS) coupling agent. To reduce the cytotoxic effect of cisplatin, the magnetic drug was then encapsulated in chitosan (CS-cisplatin-Fe3O4) through the water/oil (W/O) emulsion method. The CS-cisplatin-Fe3O4 nanoparticles were synthesized in a spherical shape with a diameter of 190 nm. The cytotoxicity assay was performed using HeLa cells. The cisplatin uptake of the cells was determined using High Performance Liquid Chromatography (HPLC) to calculate the drug content. The controlled release of cisplatin was demonstrated by regulating the dissolution and diffusion of the drug through the chitosan matrix.

Key words: Chitosan encapsulation, Magnetic nanoparticles, Cisplatin, Drug delivery

Introduction

Natural marine materials, including agar, alginates, carrageenan, and chitin, have been of great interest to researchers for their potential application within the biomedical field due to their easy accessibility and sustainable exploitation (Kurita, 2006; Laurienzo, 2010). Among various marine biomaterials, chitosan has attracted considerable attention in light of its biodegradable and bioactive properties. Chitosan is a nontoxic, biocompatible, and biodegradable amino polysaccharide that has been used in a number of medical applications, such as aqueous solutions for drug delivery (Bhattarai et al., 2010), tissue engineering (Suh and Matthew, 2000), wound dressing (Jayakumar et al., 2011), antibacterial coatings (Jena et al., 2012), and separating membranes (Mi et al., 2001). As a natural polymer, chitosan is the deacetylated derivative of chitin, which is part of the organic matrix of exoskeletons of arthropods and endoskeletons of mollusks. Thus, it is a nontoxic biocompatible amino polysaccharide that has a number of medical applications in drug release in aqueous solutions at pH < 6.5. Specifically, chitosan oligosaccharide has been applied to a variety of magnetic nanoparticles in order to enhance their colloidal stability and circulation (Zhu et al., 2009; Bae et al., 2012).

Magnetic nanoparticles (MNPs) are currently used in various medical applications, such as drug delivery (Kohler et al., 2005; Zhang et al., 2005), magnetic resonance imaging (MRI), contrast agents (Kim et al., 2003), magneto-motive ultrasound (Oh et al., 2006), and optical imaging (Oh et al., 2007). Recently, drug-loaded Fe_3O_4 NPs systems have been combined with hyperthermia treatments. These methods have the added benefit that Fe_3O_4 NPs accumulate drugs in the tar-

Received 06 October 2014; **Revised** 05 December 2014
Accepted 14 December 2014

***Corresponding Author**
E-mail: jungoh@pknu.ac.kr

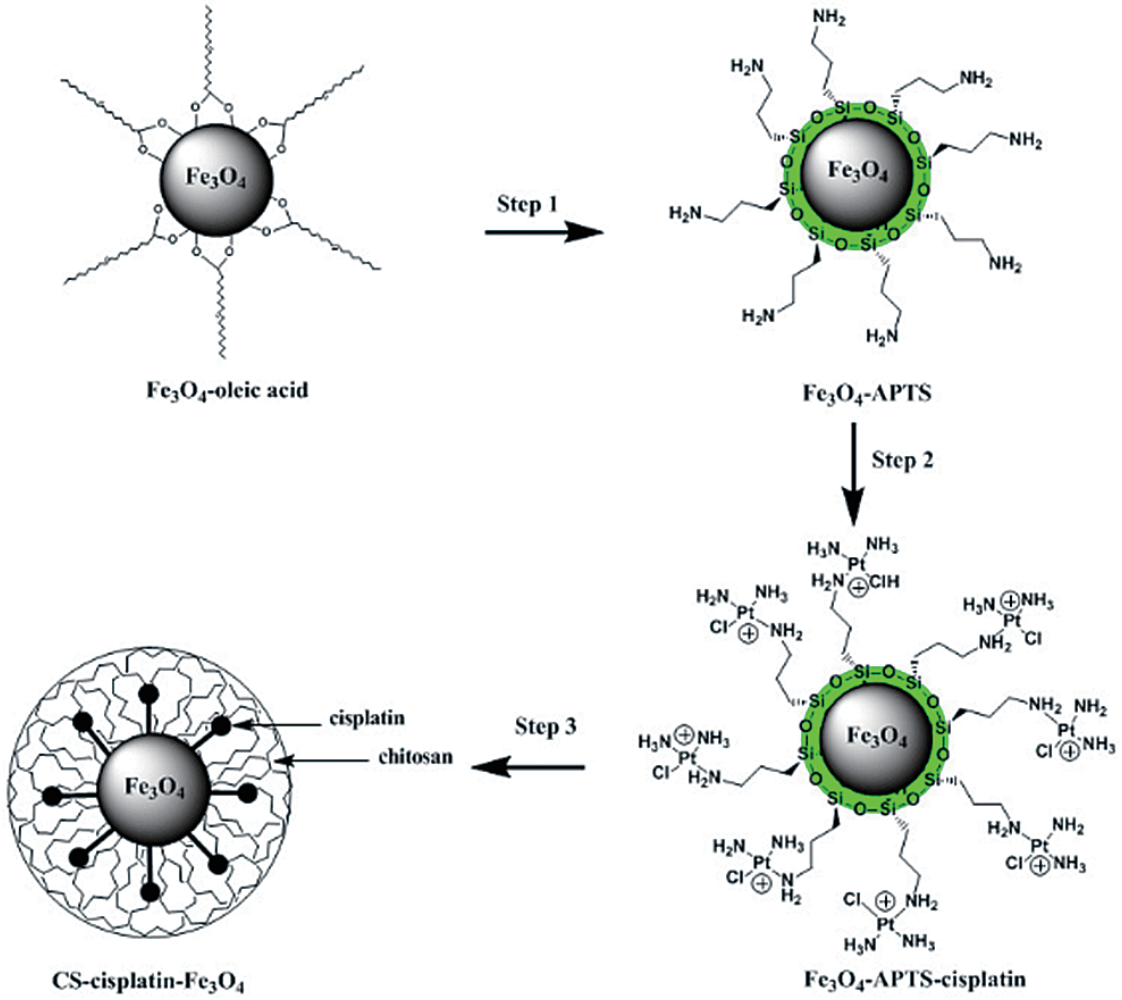

Fig. 1. Synthesis route for CS-cisplatin-Fe_3O_4. Fe_3O_4-oleic acid was synthesized via thermal decomposition method. Step 1: Oleic acid ligands were exchanged with APTS, particles became water dispersible. Step 2: APTS was used for coupling cisplatin to Fe_3O_4 NPs. Step 3: Glutaraldehyde crosslinked chitosan encapsulated Fe_3O_4-APTS-cisplatin.

geted area and generate heat in an AC magnetic field due to hysteresis loss (Ito et al., 2004). The heating of the cancer area with Fe_3O_4 NPs at 42°C can induce apoptosis of tumor cells. However, the advancement of Fe_3O_4 NPs for drug delivery for cancer purposes has been constrained due to the possibility of harmful effects on healthy cells. Therefore, the creating an efficient design that can facilitate controlled and targeted drug delivery to the specific regions of the cancer is a major challenge in drug delivery and development. Nanoparticle-based drug delivery and drug targeting systems are currently being developed to enhance the *in vivo* efficiency of anti-cancer drugs. Unfortunately, in many cases, these methods are often limited by a lack of potential drugs to reach the site of therapeutic action (Reedijk, 1999; Gonzalez et al., 2001). Considering that the cytotoxic effect of cisplatin can be harmful for healthy cells, one solution to using MNPs as drug carriers is using a polymer that can minimize drug degradation, prevent undesirable side effects, and provide controlled release of the drug (Wang et al., 1996; Ishihara et al., 2006; Kohli et al., 2007). Among the various polymers available, chitosan (CS) is one of the most widely investigated drug carriers because of its excellent mucoadhesive, nontoxic, and biodegradable properties (Onishi and Machida, 1999; Thanou et al., 2001; Sogias et al., 2008). In the present study, chitosan was employed for the delivery system of cisplatin-capped MNPs via APTS (CS-cisplain-Fe_3O_4). Chitosan encapsulation was prepared using a water/oil (W/O) emulsion method with paraffin oil as the external phase, and it was loaded with a hydrophilic magnetic drug (Arum et al., 2011). The overall schematic is presented in Fig. 1. The purpose of the present work was to develop a magnetic drug-delivery system for cisplatin coupled with chitosan encapsulation to reduce its toxic side effect and increase its affinity for specific targeting in biomedical applications. The experiment data of cell viability was obtained through the WST-1 assay for cell proliferation and viability in a 96-well format. The controlled release of cisplatin from the chitosan was assessed through a calculation of its uptake by the HeLa cells.

Materials and Methods

Materials

Cis-diamminedichloroplatinum(II) (cisplatin), chitosan (deacetylation 85%, Mn 50 KDa, viscosity 20-300 cP), $FeCl_3 \cdot 6H_2O$ (98%), oleic acid (90%), 1-octadecene (90%), (3-Aminopropyl)-trimethoxysilane (APTS), tetramethylammonium hydroxide (TMAH), hydrochloric acid (37%), isopropanol, Span 80, Tween-20, and glutaraldehyde (25%) were purchased from Sigma-Aldrich Chemical Co. Sodium oleate (95%) was obtained from TCI (Korea). Petroleum ether and sodium chloride were produced by Samchun Chemicals (Korea). All chemicals were analytical grade reagents and used directly without further purification.

Synthesis of cisplatin-capped Fe_3O_4 NPs via APTS

The synthesis of Fe_3O_4 NPs was performed following the reported procedure (Park et al., 2004). Water-soluble Fe_3O_4 -APTS were prepared with the two-step silanization process (De Palma et al., 2007) with little modification. APTS was used to couple cisplatin to Fe_3O_4 NPs. 10 mg of Fe_3O_4-APTS was dispersed in 10 mL of ethyl alcohol and 500 mL of TMAH 1 M (pH adjusted to 8). In the other container, 20 mg of cisplatin was dissolved in 500 mL of HCl 0.2 M and heated with a water bath at 80°C several times. The solution was then added to a flask containing Fe_3O_4-APTS and stirred for 24 h. After reaction, Fe_3O_4-APTS-cisplatin was collected with a permanent magnet. The purification of the conjugation from the free cisplatin was performed by dialysis in 0.9% sodium chloride solution with a cellulose membrane (MWCO=7,000 Da) for three days. The Fe_3O_4-APTS-cisplatin was then dried under a vacuum at 85°C for 3 h.

Synthesis of CS-cisplatin-Fe_3O_4

The typical water-in-oil (W/O) emulsion method was used to produce CS-Cisplatin-Fe_3O_4. 20 mg of CS was dissolved in 3 mL of acetic 1% acid. 10 mg of Fe_3O_4-APTS-cisplatin was dissolved in 0.5 mL of water and treated with ultrasonic waves for 10 min. These solutions were added dropwise into 60 mL of paraffin oil containing emulsion stabilizer 5% Span 80 and 0.5% Tween-20 under a stirring rate of 1,200 rpm at room temperature. After 24 h, the suspension was added with 2 mL glutaraldehyde 25% and stabilized for 3 h. The CS-Cisplatin-Fe_3O_4 was then collected by applying a permanent magnet, washed three times using petroleum ether, and recovered by centrifugation at 10,000 rpm. The final product was washed with isopropanol and dried under a vacuum at 70°C for 12 h.

Characterization techniques

The crystalline structure of the Fe_3O_4 NPs was examined with XRD (Philips, X'Pert-MPD System, Netherlands); the changes in the chemical groups present in the nanoparticles were monitored using a FTIR spectrometer (Jasco FT/IR 4100, USA); the attachment of cisplatin to APTS-Fe_3O_4 NPs was detected with XPS (Thermo VG Scientific, MultiLab2000, England); the particle size was measured using TEM (Jeol, JEM-2010, Japan); the particle shapes were observed with SEM (Hitachi, S-2400, Japan); the zeta potential was determined using a Electrophoretic Light Scattering Spectrophotometer (Otsuka Electronics, ELS-8000, Japan); and the magnetic properties were measured using SQUID (Quantum Design, MPMS XL 7.0, USA).

Drug content in nanoparticles

Fe_3O_4-APTS-cisplatin and CS-cisplatin- Fe_3O_4 NPs were dissolved in nitric acid (pH 3.5) at a concentration of 100 μg/mL. Subsequently, the samples were sonicated for 60 min and centrifuged at 8,000 rpm for 10 min. The supernatants were measured using HPLC. The cisplatin standard solution was prepared in 0.9% NaCl solution and used to prepare the calibration curves ranging from 1 to 10 μg/mL. The drug content was calculated using the following Eq. 1:

$$drug\ content = \frac{amount\ drug\ in\ nanoparticles}{amount\ of\ nanoparticles} \times 100\% \quad (1)$$

Chromatography condition

A Flexar HPLC system (PerkinElmer, USA) was used for the liquid chromatography system. A 20-μL sample was injected into the C18 column, 150 × 4.6 mm, 5 μm particle size (Agilent Eclipse XDB, USA). The mobile phase was a mixture of water/methanol/acetonitrile (50:25:25), and the detection was performed at 254 nm with a running time of 20 min.

Cell culture and viability

The HeLa cells (ATCC CCL-2) were cultured in Dulbecco's modified Eagle's medium (DMEM, Thermo Scientific, USA) and supplemented with 10% fetal bovine serum (FBS, Thermo Scientific). The cells were incubated at 37°C in a humidified atmosphere of 5% CO_2 and 95% air, and the growth medium was changed twice a week. The cell seeding was performed by removing the medium and adding 2 mL of Trypsin (0.25%)-EDTA (0.53 mM) (Thermo Scientific) to the flask, then observing the cells under a microscope until the cell layer was dispersed. Finally, a 6-ml medium was added, and the cultures were incubated at 37°C.

The cytotoxicity of the CS-cisplatin-MNPs was measured using the WST-1 assay (ITSBio, Korea). The HeLa cells were seeded at a density of 1.0×10^5 cells/well plates and incubated for 24 h. Fe_3O_4-APTS, Fe_3O_4-APTS-cisplatin, chitosan-glutaraldehyde, CS-cisplatin-Fe_3O_4, and cisplatin

(each with a concentration of 50 mg/mL) were added to the culture media in the plate, and the untreated cells were used as controls. The cells were incubated in humidified 5% CO_2 at 37°C for 12, 24, or 48 h, respectively. At the end of the incubation time, 10-μL WST-1 solution was added to each well plate. After 4 h of incubation, the plates were shaken for 1 m, and the absorbance peak at 450 nm was measured and calculated with Eq. 2 using a microtiter plate reader (Molecular Device, USA).

$$Cell\ viability = \frac{mean\ test\ wells}{mean\ control\ wells} \times 100\% \quad (2)$$

In vitro release of cisplatin and drug uptake

The amount of cisplatin released and the uptake into the HeLa cells was determined using HPLC, as reported earlier (Lopez-Flores et al., 2005). The HeLa cells (1.0×10^6 cells/well) were treated with CS-cisplatin-Fe_3O_4 with a final concentration of 50 μg/mL and were incubated for 3, 6, or 12 h in a 5% CO_2 atmosphere at 37°C. The untreated cells samples were incubated for the same period. After incubation, the cells were washed with PBS and harvested with 500 μL of trypsin containing EDTA. Subsequently, they were lysed with buffer (Tris 100 mM, EDTA 5 mM, NaCl 200 mM, 0.2% SDS at pH 8) for three hours at 55°C. The homogenate was filtered and extracted with 80 μL of chloroform by vortexing at the maximum speed for one minute on a Vortex-Genie (Scientific Industries, USA), and then separated by centrifugation at 10,000 rpm for 5 min. Finally, 20 μL of the chloroform layer was injected into the HPLC system under the same chromatographic conditions.

Results

Characterization of Fe_3O_4 NPs

The spherical monodisperse iron oxide nanoparticle was prepared through thermal decomposition of Fe-oleate in the presence of oleic acid as a surfactant. Fig. 2 represents the XRD patterns of Fe_3O_4 at 2θ = 30.3, 35.5, 36.5, 42.5, 57.0, 62.2, and 73.4, corresponding to 220, 311, 400, 511, 440, and 533 Bragg reflection planes, which were observed in all of the samples. These peaks are consistent with the standard pattern of Fe_3O_4 (JCPDS no. 79-0418) with a cubic inverse spinel structure. The results indicated that the crystal structure of Fe_3O_4 NPs was not changed during the modification with oleic acid. The mean crystal sizes were determined by the Debye–Scherrer equation with XRD data, $D = K\lambda/(\beta\cos\theta)$, where K is a constant (K = 0.94 for Cu-Kα), λ is the wavelength (0.15405 nm for Cu-Kα), β is the peak width of the half-maximum, and θ is the diffraction angle (Sun et al., 2009). Thus, the crystal sizes of the Fe_3O_4 NPs were found to be approximately 14.25 nm. To confirm the relative surface composition of the functionalized Fe_3O_4 NPs, XPS was used, as shown in Fig. 3a. The binding energy of $Fe_{2p3/2}$ and $Fe_{2p1/2}$ were 711.1 eV and 724.5 eV, respectively, which are close to the standard data of Fe_3O_4.

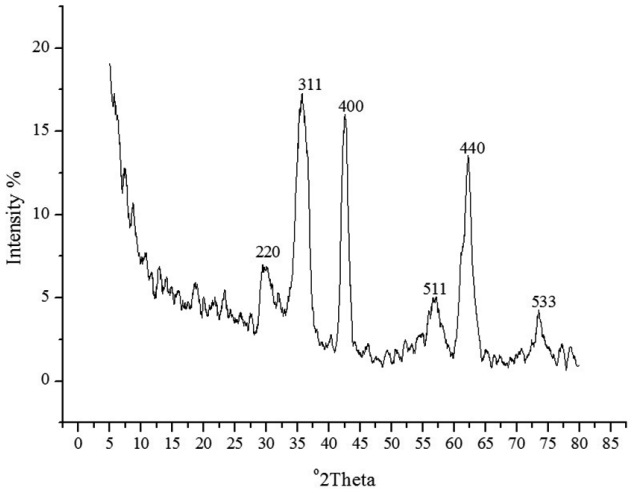

Fig. 2. X-ray diffraction pattern of Fe_3O_4-oleic acid NPs.

Characterization of Fe_3O_4-APTS-cisplatin

The presence of oleic acid on the surface of Fe_3O_4 NPs from the above result caused the particles to become hydrophobic. APTS functionalized the Fe_3O_4 NPs to modify the particle to become hydrophilic. As previously established, silane can be applied to exchange the original hydrophobic oleic acid ligand from the surface of the Fe_3O_4 NPs and increase biocompatibility (Jana et al., 2007). The influence of the end group of the APTS coating gave the nanoparticles a water-dispersible effect. In the next step, APTS was used to couple cisplatin to Fe_3O_4 NPs through a nucleophilic substitution reaction between the chloride ligand and the amino group of the silane. The XPS data of Fe_3O_4-APTS-cisplatin is shown in Fig. 3a. The binding energy of Si_{2s} and Si_{2p} were found as 156.4 and 105.4 eV, respectively, which are similar to the previous data of silane (Wu and Xu, 2005). The peaks of C_{1s} at 290.9 eV are close to the standard data of alkyl chains, signifying it derived from the alkyl chain of APTS. The binding energy of N_{1s} was 404.0 eV, which is close to the standard data of an amine group. The presence of cisplatin on the surface of the MNPs is shown through the peak of Pt_{4f} at 78.6 eV and Cl_{2p} at 201.7 eV. In order to verify the bond between APTS and cisplatin, the platinum peak was compared with the Pt_{4f} peak of the cisplatin standard solution. The results showed there were shifts in the position of the peaks to lower energy values of 73.11 and 76.44 eV for the cisplatin standard solution (Fig. 3c) and to 72.49 and 75.75 eV for the Fe_3O_4-APTS-cisplatin (Fig. 3b). These lower energies indicated a change in the binding state of the platinum. As previously reported, the particles

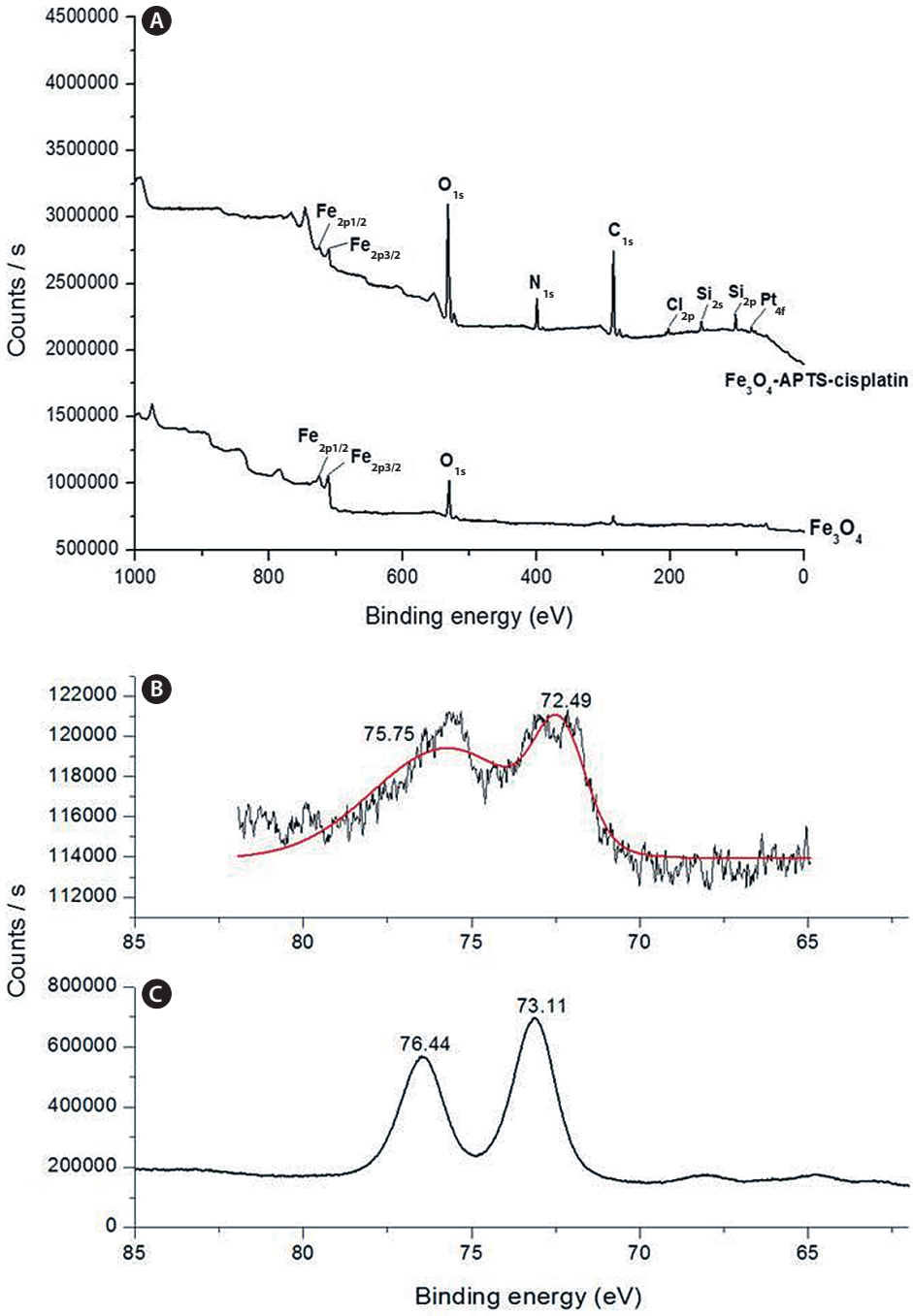

Fig. 3. (A), XPS spectra of Fe_3O_4 NPS and Fe_3O_4-APTS-cisplatin; (B), Pt_{4f} peaks of Fe_3O_4-APTS-cisplatin; (C), Pt_{4f} peaks of pure cisplatin.

become less polar as many platinum-bound chlorines could be substituted by the terminal amine group of APTS (Bhowmick et al., 2010).

Characterization of CS-cisplatin-Fe_3O_4

The typical FT-IR spectra of Fe_3O_4 NPs are shown in Fig. 4a. The C=O at 1,711 cm^{-1}, the C-H stretch at 2,911 cm^{-1}, and the CH_2/CH_3 bending at 1,464 cm^{-1} are evidence of oleic acid-coated Fe_3O_4 NPs. Fig. 4b shows the FT-IR of Fe_3O_4-APTS. The peaks at around 1,638 cm^{-1} were ascribed to the $–NH_2$ terminal of APTS, and the Si-O-Si bridges were found at 1,098 cm^{-1}. The absence of oleic acid peaks and appearance of silane peaks in the Fe_3O_4 NPs indicate that the ligand exchange was performed successfully. The FT-IR peaks of CS-cisplatin-

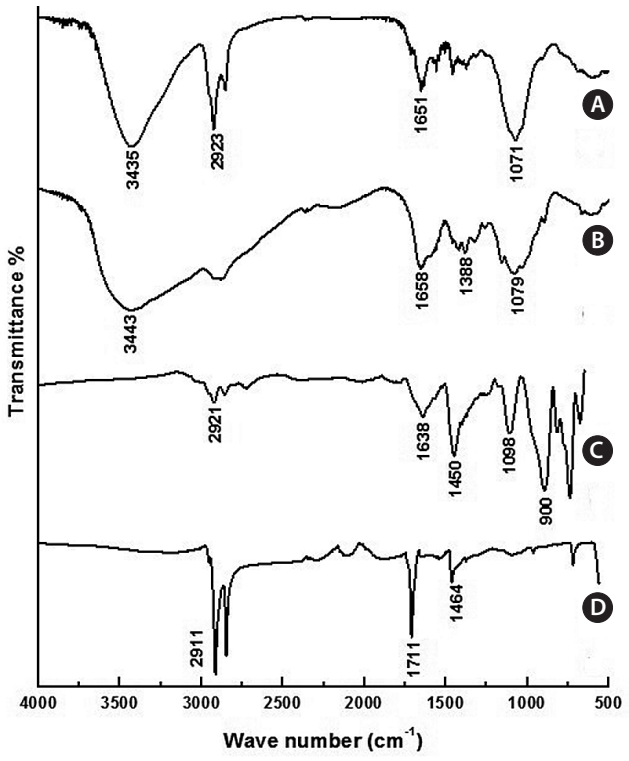

Fig. 4. FT-IR spectra of (A), Fe_3O_4-oleic acid; (B), Fe_3O_4-APTS; (C), chitosan standard; and (D), CS-cisplatin-Fe_3O_4.

Fe_3O_4 (Fig. 4d) were compared with those of pure chitosan (Fig. 4c). The same pattern was shown for the O-H region in 3,435cm^{-1} and the C-O stretching at 1,071 cm^{-1}. In the case of CS-cisplatin-Fe_3O_4 (Fig. 4d), a sharp peak was observed at 1,651 cm^{-1} that derived from the glutaraldehyde imine group (C=N). The reaction between chitosan and glutaraldehyde made the amino group of chitosan convert into an imine group (C=N). The strong peak of the C-H stretch at 2,923 cm^{-1} resulted from the alkane groups of APTS.

TEM characterizations

Fig. 5 shows a TEM image of all processes of magnetic nanoparticles, and the size was measured by ImageJ software. Fig. 5a shows Fe_3O_4-oleic acid, and the diameter was 14.5 nm, which is close to the calculation using the Debye–Scherrer equation in our XRD data. Fig. 5b shows the Fe_3O_4-APTS nanoparticles were spherical and 15.87 nm in size, and they did not appear to aggregate in water. Cisplatin-capped Fe_3O_4 via an APTS coupling agent with an average size of 8.8 nm can be seen in Fig. 5c. Dark spots at the Fe_3O_4 NPs surface were indicative of cisplatin. Furthermore, the TEM image of CS-cisplatin Fe_3O_4 (Fig. 5d) shows the effect of glutaraldehyde crosslinking amine functional groups of chitosan, which had a spherical shape and diameter of 190 nm.

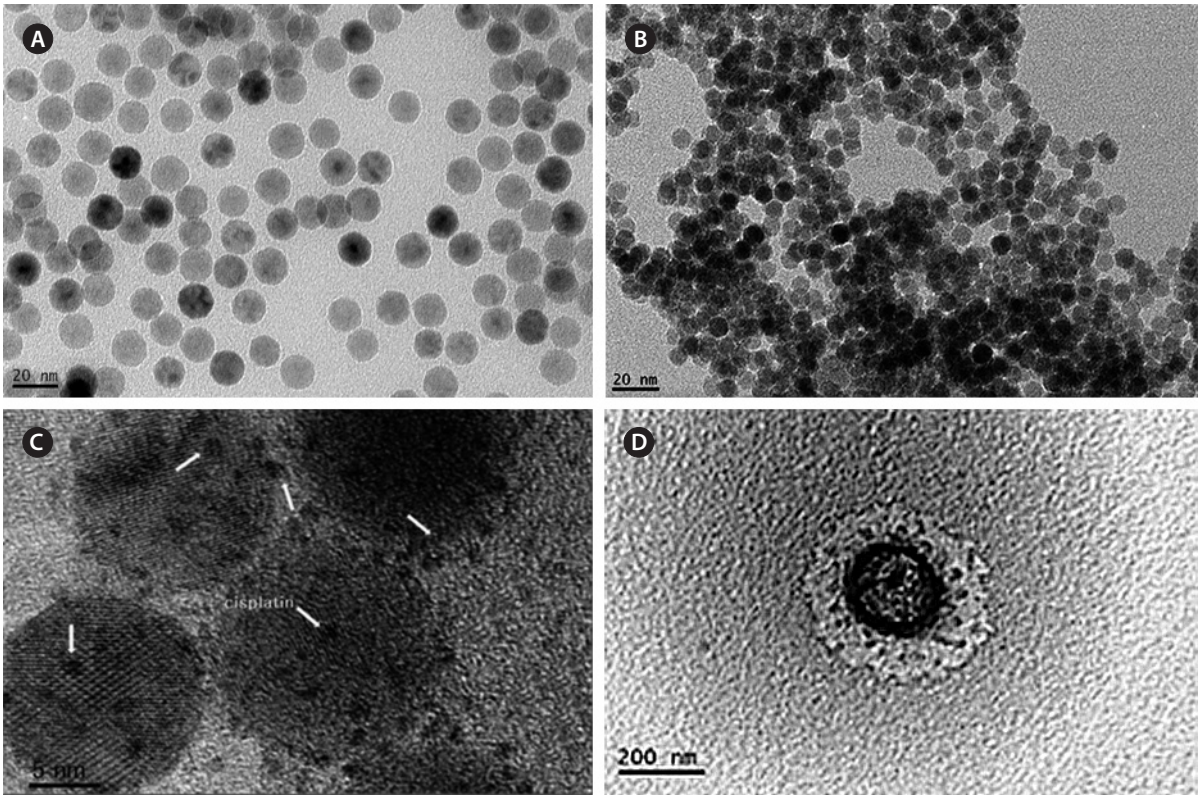

Fig. 5. TEM images (A), Fe_3O_4-oleic acid; (B), Fe_3O_4-APTS; (C), Fe_3O_4-APTS-cisplatin; (D), CS-cisplatin-Fe_3O_4.

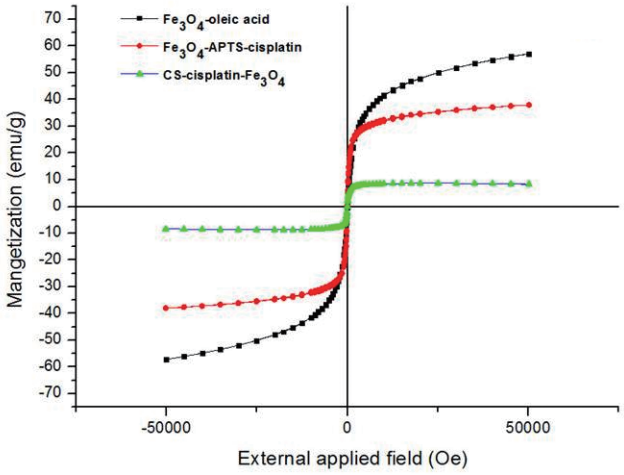

Fig. 6. Magnetic hysteresis for Fe_3O_4-oleic acid (■), Fe_3O_4-APTS-cisplatin (●), and CS-cisplatin-Fe_3O_4 (▲) at room temperature.

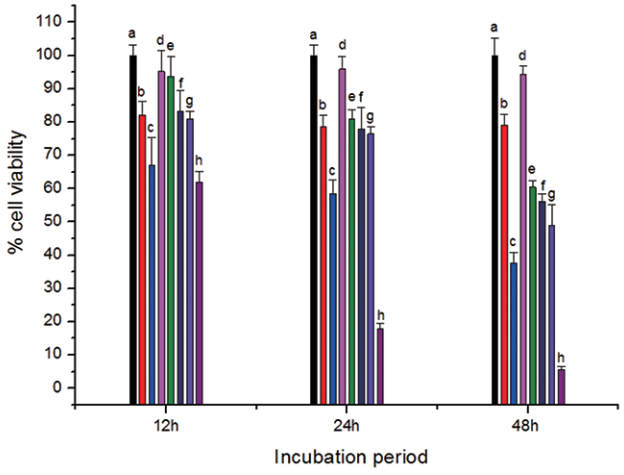

Fig. 8. *In vitro* cell viability of control (a), Fe_3O_4-APTS; (b), Fe_3O_4-APTS-cisplatin; (c), chitosan; (d), CS-cisplatin-Fe_3O_4 50 μg/mL; (e), CS-cisplatin-Fe_3O_4 75 μg/mL; (f), CS-cisplatin-Fe_3O_4 100 μg/mL; (g) and cisplatin; (h) in HeLa cells after 12, 24, and 48 h. Error bars represent standard deviations.

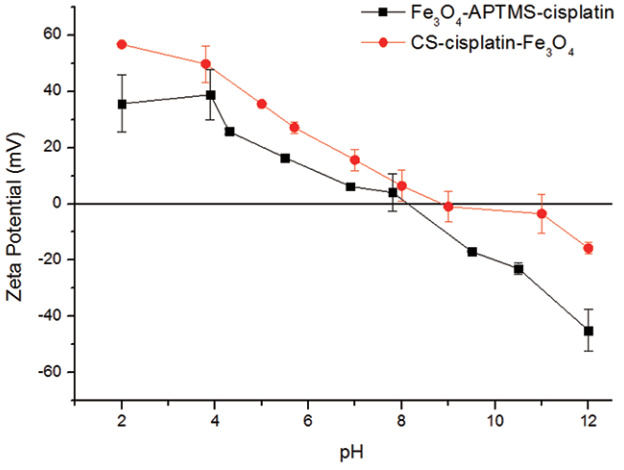

Fig. 7. pH-dependent zeta potential curves of Fe_3O_4-APTS-cisplatin and CS-cisplatin-Fe_3O_4. Error bars in the figures represent standard deviations.

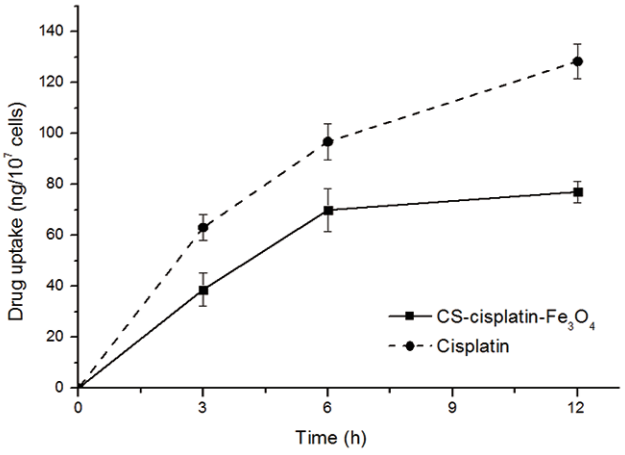

Fig. 9. Time-dependent drug uptake by HeLa cells. Data represent the average values ± SD of three separate experiments.

Magnetic properties measured by SQUID

Fig. 6 shows the magnetic curves as a function of applied field at 300K obtained for dry powders of Fe_3O_4-oleic acid, Fe_3O_4-APTS-cisplatin, and CS-cisplatin-Fe_3O_4, respectively. The magnetization saturations were found to be 57.2 emu/g for Fe_3O_4-oleic acid, 38.0 emu/g for Fe_3O_4-APTS-cisplatin, and 8.5 emu/g for CS-cisplatin-Fe_3O_4. The magnetization value decreased after coating due to the existence of silane and chitosan, which formed polymerized multilayers. In addition, no hysteresis was found in any of the samples, indicating that these nanoparticles have superparamagnetic properties.

Drug content and zeta potential

The percentages of cisplatin content (m/v) in the nanoparticles are shown in Table 1. Cisplatin content in Fe_3O_4-APTS was 27%, while in the Fe_3O_4-CS system, it was 18%. The amount of cisplatin seems to be influenced by the amount of iron encapsulated by chitosan. The measured zeta potential values of these particles are shown in Fig. 7.

It is shown that Fe_3O_4-APTS-cisplatin and CS-cisplatin-Fe_3O_4 were both positively charged at acidic pH, which confirms the presence of amino groups on the particles in their protonated form and thus confirms the presence of chitosan

Table 1. Drug content of Fe_3O_4-APTS-cisplatin and CS-cisplatin-Fe_3O_4

Delivery system	Cisplatin content (%)
Fe_3O_4-APTS-cisplatin	27
CS-cisplatin-Fe_3O_4	18

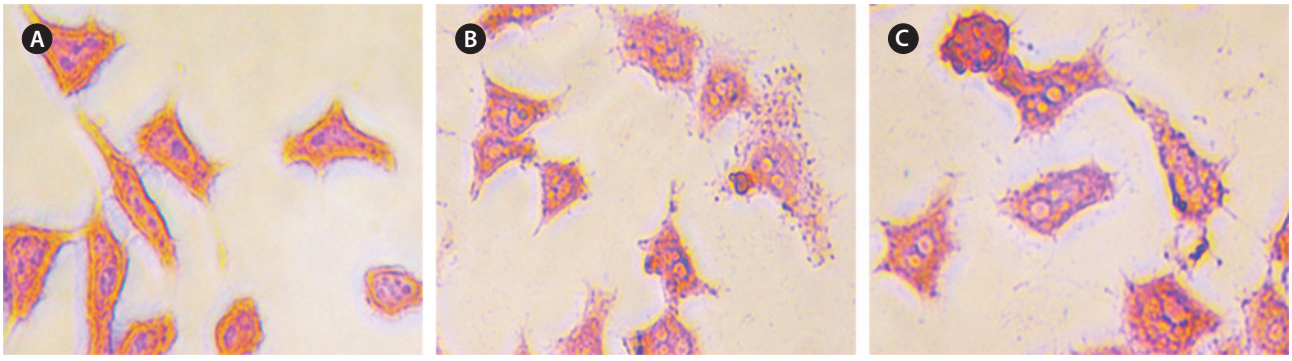

Fig. 10. Prussian blue-stained HeLa cells after 48-h treatment with CS-cisplatin-Fe_3O_4 NPs. Control cell (A), 25 μg/L concentration (B), and 50 μg/mL concentration (C).

on the particle surface. In the case of CS-cisplatin-Fe_3O_4, it was observed that the surface potential indicated precipitation starting from pH 6.0 and decreased to 0 at around pH 9, indicating the amino groups were deprotonated. However, the pKa of chitosan was 6.5, and when the pH increased, chitosan lost its protonated amino group, promoting intramolecular hydrogen bonding and causing the chitosan to precipitate.

In vitro cell viability assay

The toxicity of CS-cisplatin-Fe_3O_4 was demonstrated by a WST-1 cytotoxicity assay. This assay is based on the cleavage of the tetrazolium salt to water-soluble formazan by the succinate-tetrazolium reductase system, which belongs to the respiratory chain and is only in the viable cells (Ishiyama et al., 1996). Therefore, the amount of formazan dye is directly related to the number of living cells. Cell viability was observed after cells were incubated for various time periods: 12, 24, and 48 h. Fig. 8 shows that cell viability decreased more rapidly for cisplatin and Fe_3O_4-APTS-cisplatin. As confirmed by previous literature (Jamieson and Lippard, 1999), cisplatin can promote abnormal linkages in DNA through chloride ligand crosslinking and hydrogen bonding of amine ligands. In the case of Fe_3O_4-APTS-cisplatin, the cytotoxic action came from the one chloride ligand remaining and the hydrogen-bonding interaction of the NH_2R group to the oxygen-phosphate of DNA (Komeda et al., 2011). The cell viability of Fe_3O_4-APTS and chitosan appeared stable for all incubation periods. Neither had a significant effect on cell viability, and both were categorized as non-toxic. For CS-cisplatin-Fe_3O_4, viability declined during incubation times, indicating that cisplatin was continually released. However, the glutaraldehyde crosslink chitosan microsphere demonstrated minimal cisplatin toxicity.

In vitro release of cisplatin

The intracellular platinum concentrations increased continuously as a consequence of DNA-platination. In order to demonstrate the effect of chitosan on controlling drug release, we compared the cell-uptake behavior to a cisplatin drug with the same concentration of cisplatin content in its nanoparticles. Fig. 9 indicates that cisplatin accumulation within HeLa cells was more accelerated. The drug-release rate from the glutaraldehyde crosslinked chitosan microsphere was controlled by the dissolution and diffusion of the drug from the chitosan matrix (Wang et al., 1996).

Cell labeling

Intracellular Prussian blue staining was used to demonstrate the presence of ferric iron in the cytological preparations of HeLa cell suspensions after 48 h incubation. Fig. 10 shows obvious visual evidence of the presence of iron in panels (b) and (c) compared with untreated cells (a), and the amount of iron was increased for higher concentrations of CS-cisplatin-Fe_3O_4 MNPs.

The present work proposed a method for developing a magnetic drug-delivery system for cisplatin intended to be used in specifically targeted cancer therapy. In our synthesis procedure, we kept the morphology of the nanoparticles in a spherical shape. For biomedical applications, it is crucial that magnetic nanoparticles are spherical in shape and uniform in size. The spherical shape enables the uniform immobilization of bioactive molecules onto the surfaces of the particles, and the uniform size endows the particles with uniform magnetic properties. We used chitosan encapsulation to optimize the pharmaceutical action while reducing the cytotoxicity of cisplatin. In addition, to prepare a slow-release system, we controlled cisplatin from the chitosan microsphere, which can be observed in the intracellular concentration–time profiles (Fig. 9), and chitosan was shown to reduce the release rate of cisplatin. In conclusion, our results support the idea that chitosan nanoparticles are a suitable carrier for controlled release and a magnetic drug-delivery system using cisplatin and that they should be promoted for further gene-based therapy and magnetic hyperthermia.

Acknowledgments

This work was supported by a research grant from Pukyong National University (2013).

Reference

Arum Y, Song Yand Oh J. 2011. Controlling the optimum dose of AMPTS functionalized-magnetite nanoparticles for hyperthermia cancer therapy. Appl Nanosci 1, 237-246.

Bae KH, Park M, Do MJ, Lee N, Ryu JH, Kim GW, Kim C, Park TG and Hyeon T. 2012. Chitosan oligosaccharide-stabilized ferrimagnetic iron oxide nanocubes for magnetically modulated cancer hyperthermia. ACS nano 6, 5266-5273.

Bhattarai N, Gunn J and Zhang M. 2010. Chitosan-based hydrogels for controlled, localized drug delivery. Adv Drug Deliv Rev 62, 83-99.

Bhowmick T, Yoon D, Patel M, Fisher J and Ehrman S. 2010. In vitro effects of cisplatin-functionalized silica nanoparticles on chondrocytes. J Nanopart Res 12, 2757-2770.

De Palma R, Peeters S, Van Bael MJ, Van den Rul H, Bonroy K, Laureyn W, Mullens J, Borghs G and Maes G. 2007. Silane ligand exchange to make hydrophobic superparamagnetic nanoparticles water-dispersible. Chem Mater 19, 1821-1831.

Gonzalez VM, Fuertes MA, Alonso C and Perez JM. 2001. Is cisplatin-induced cell death always produced by apoptosis? Molec Pharmacol 59, 657-663.

Ishihara M, Obara K, Nakamura S, Fujita M, Masuoka K, Kanatani Y, Takase B, Hattori H, Morimoto Y, Ishihara M, Maehara T and Kikuchi M. 2006. Chitosan hydrogel as a drug delivery carrier to control angiogenesis. J Artific Org : Offic J Japanese Soc Artific Org 9, 8-16.

Ishiyama M, Tominaga H, Shiga M, Sasamoto K, Ohkura Y and Ueno K. 1996. A combined assay of cell viability and in vitro cytotoxicity with a highly water-soluble tetrazolium salt, neutral red and crystal violet. Biol Pharmac Bull 19, 1518-1520.

Ito A, Kuga Y, Honda H, Kikkawa H, Horiuchi A, Watanabe Y and Kobayashi T. 2004. Magnetite nanoparticle-loaded anti-HER2 immunoliposomes for combination of antibody therapy with hyperthermia. Cancer lett 212, 167-175.

Jamieson ER and Lippard SJ. 1999. Structure, recognition, and processing of cisplatin-DNA adducts. Chem Rev 99, 2467-2498.

Jana NR, Earhart C and Ying JY. 2007. Synthesis of water-soluble and functionalized nanoparticles by silica coating. Chem Mater 19, 5074-5082.

Jayakumar R, Prabaharan M, Sudheesh Kumar PT, Nair SV and Tamura H. 2011. Biomaterials based on chitin and chitosan in wound dressing applications. Biotechnol Advanc 29, 322-337.

Jena P, Mohanty S, Mallick R, Jacob B and Sonawane A. 2012. Toxicity and antibacterial assessment of chitosan-coated silver nanoparticles on human pathogens and macrophage cells. Intern J Nanomedic 7, 1805-1818.

Kim DK, Mikhaylova M, Wang FH, Kehr J, Bjelke B, Zhang Y, Tsakalakos T and Muhammed M. 2003. Starch-coated superparamagnetic nanoparticles as MR contrast agents. Chem Mater 15, 4343-4351.

Kohler N, Sun C, Wang J and Zhang M. 2005. Methotrexate-modified superparamagnetic nanoparticles and their intracellular uptake into human cancer cells. Langmuir : ACS J Surfac Coll 21, 8858-8864.

Kohli E, Han HY, Zeman AD and Vinogradov SV. 2007. Formulations of biodegradable Nanogel carriers with 5'-triphosphates of nucleoside analogs that display a reduced cytotoxicity and enhanced drug activity. J Contr Rel : Offic J Contr Rel Soc 121, 19-27.

Komeda S, Moulaei T, Chikuma M, Odani A, Kipping R, Farrell NP and Williams LD. 2011. The phosphate clamp: a small and independent motif for nucleic acid backbone recognition. Nucl Acid Res 39, 325-336.

Kurita K. 2006. Chitin and chitosan: functional biopolymers from marine crustaceans. Mar Biotechnol 8, 203-226.

Laurienzo P. 2010. Marine polysaccharides in pharmaceutical applications: an overview. Mar Drug 8, 2435-2465.

Lopez-Flores A, Jurado R and Garcia-Lopez P. 2005. A high-performance liquid chromatographic assay for determination of cisplatin in plasma, cancer cell, and tumor samples. J Pharmacol Toxicol Meth 52, 366-372.

Mi FL, Shyu SS, Wu YB, Lee ST, Shyong JY and Huang RN. 2001. Fabrication and characterization of a sponge-like asymmetric chitosan membrane as a wound dressing. Biomaterials 22, 165-173.

Oh J, Feldman MD, Kim J, Condit C, Emelianov S and Milner TE. 2006. Detection of magnetic nanoparticles in tissue using magneto-motive ultrasound. Nanotechnology 17, 4183-4190.

Oh J, Feldman MD, Kim J, Kang HW, Sanghi P and Milner TE. 2007. Magneto-motive detection of tissue-based macrophages by differential phase optical coherence tomography. Laser Surger Medic 39, 266-272.

Onishi H and Machida Y. 1999. Biodegradation and distribution of water-soluble chitosan in mice. Biomaterials 20, 175-182.

Park J, An K, Hwang Y, Park JG, Noh HJ, Kim JY, Park JH, Hwang NM and Hyeon T. 2004. Ultra-large-scale syntheses of monodisperse nanocrystals. Nat Mater 3, 891-895.

Reedijk J. 1999. Why does Cisplatin reach Guanine-n7 with competing s-donor ligands available in the cell? Chem Rev 99, 2499-2510.

Sogias IA, Williams AC and Khutoryanskiy VV. 2008. Why is chitosan mucoadhesive? Biomacromolecules 9, 1837-1842.

Suh JK and Matthew HW. 2000. Application of chitosan-based polysaccharide biomaterials in cartilage tissue engineering: a review. Biomaterials 21, 2589-2598.

Sun X, Zheng C, Zhang F, Yang Y, Wu G, Yu A and Guan N. 2009. Size-Controlled Synthesis of Magnetite (Fe3O4) Nanoparticles coated with glucose and gluconic acid from a single Fe(III) precursor by a sucrose bifunctional hydrothermal method. J Physic Chem C 113, 16002-16008.

Thanou M, Verhoef JC andJunginger HE. 2001. Oral drug absorption enhancement by chitosan and its derivatives. Advanc Drug Deliv Rev 52, 117-126.

Wang YM, Sato H, Adachi I and Horikoshi I. 1996. Optimization of the formulation design of chitosan microspheres containing cisplatin. J Pharmac Sci 85, 1204-1210.

Wu P and Xu Z. 2005. Silanation of nanostructured mesoporous mag-

netic particles for heavy metal recovery. Indus Engineer Chem Res 44, 816-824.

Zhang JQ, Zhang ZR, Yang H, Tan QY, Qin SR and Qiu XL. 2005. Lyophilized paclitaxel magnetoliposomes as a potential drug delivery system for breast carcinoma via parenteral administration: in vitro and in vivo studies. Pharmac Res 22, 573-583.

Zhu L, Ma J, Jia N, Zhao Y and Shen H. 2009. Chitosan-coated magnetic nanoparticles as carriers of 5-fluorouracil: preparation, characterization and cytotoxicity studies. Coll Surf B, Biointerfaces 68, 1-6.